communications earth & environment

Article

https://doi.org/10.1038/s43247-024-01516-2

A scalable big data approach for remotely tracking rangeland conditions

Zunyi Xie [1,2,3] ✉, Edward T. Game[4], Stuart R. Phinn [2], Matthew P. Adams[5,6,7,8], Yunden Bayarjargal[9], David J. Pannell[10], Ganbold Purevbaatar[9], Batkhuyag Baldangombo[9], Richard J. Hobbs[11], Jing Yao[12] & Eve McDonald-Madden [2]

Rangelands, covering half of the global land area, are critically degraded by unsustainable use and climate change. Despite their extensive presence, global assessments of rangeland condition and sustainability are limited. Here we introduce a novel analytical approach that combines satellite big data and statistical modeling to quantify the likelihood of changes in rangeland conditions. These probabilities are then used to assess the effectiveness of management interventions targeting rangeland sustainability. This approach holds global potential, as demonstrated in Mongolia, where the shift to a capitalist economy has led to increased livestock numbers and grazing intensity. From 1986 to 2020, heavy grazing caused a marked decline in Mongolia's rangeland condition. Our evaluation of diverse management strategies, corroborated by local ground observations, further substantiates our approach. Leveraging globally available yet locally detailed satellite data, our proposed condition tracking approach provides a rapid, cost-effective tool for sustainable rangeland management.

Rangelands, extensively managed grazing lands usually dominated by natural or semi-natural non-forest vegetation[1], occupy around half of the world's land surface (Fig. 1). They provide important ecosystem services to society including cultural identity, livestock forage, climate, and disease regulation[2]. Indeed, inexpensive rangeland feed is critical to the global production of affordable meat, milk products, leather, and wool[3]. Over 2.7 billion people live in or are supported by rangelands, a large proportion of which are in Low- and Middle-Income Countries[4] (Fig. 1). Rangelands also provide habitat for thousands of threatened, unique, and often wide-ranging species (Fig. 1). For example, there are over 1000 threatened species living in the Australian rangelands according to the latest International Union for Conservation of Nature (IUCN) Red List[5].

The importance of rangelands to people places them under increasing pressure from unsustainable land practices, which with other stressors such as climate change and invasive species, have led to their severe land degradation over many parts of the world (Fig. 1). Many rangelands have turned to dust after loss of perennial grasses and subsequent erosion (e.g., fast increasing bare ground in northern Kenyan rangelands since 1990[6]). Degradation-induced loss of rangelands not only threatens the natural world, the plants and animals that depend on rangeland habitats, but also the ecological well-being, economic prosperity, and cultural diversity of the global human community[7]. It thus hampers our ability to reach multiple Sustainable Development Goals (SDGs) including poverty alleviation, food security, and protecting biodiversity on land.

Assessing the current state and temporal dynamics of rangelands is crucial for their sustainable management and conservation. While satellite imagery has been leveraged for these insights, the applications of such methods often involve compromises between temporal coverage, spatial resolution, and geographic scope (refer to Table S1). For instance, the US Rangeland Analysis Platform (US RAP) utilizes the comprehensive Landsat archive to provide moderate-resolution (30 m) annual mapping from 1984 to 2017 across the USA[8]. Its expansion beyond American regions is constrained by the machine learning approach's need for extensive field data as training samples. In contrast, the Australian Rangeland and Pasture

[1]College of Geography and Environmental Science, Henan University, Kaifeng 475004, China. [2]School of Earth and Environmental Sciences, The University of Queensland, Brisbane, QLD 4072, Australia. [3]Key Laboratory of Geospatial Technology for the Middle and Lower Yellow River Regions, Ministry of Education, Henan University, Kaifeng 475004, China. [4]The Nature Conservancy, Brisbane, QLD 4101, Australia. [5]School of Mathematical Sciences, Queensland University of Technology, Brisbane, QLD 4000, Australia. [6]Centre for Data Science, Queensland University of Technology, Brisbane, QLD 4000, Australia. [7]ARC Centre of Excellence for Mathematical and Statistical Frontiers, Queensland University of Technology, Brisbane, QLD 4000, Australia. [8]School of Chemical Engineering, The University of Queensland, Brisbane, QLD 4072, Australia. [9]The Nature Conservancy Mongolia, Ulaanbaatar 21401, Mongolia. [10]School of Agriculture and Environment, The University of Western Australia, Perth, WA 6009, Australia. [11]School of Biological Sciences, The University of Western Australia, Perth, WA 6009, Australia. [12]Urban Big Data Centre, University of Glasgow, Glasgow, UK. ✉e-mail: zunyixie@henu.edu.cn

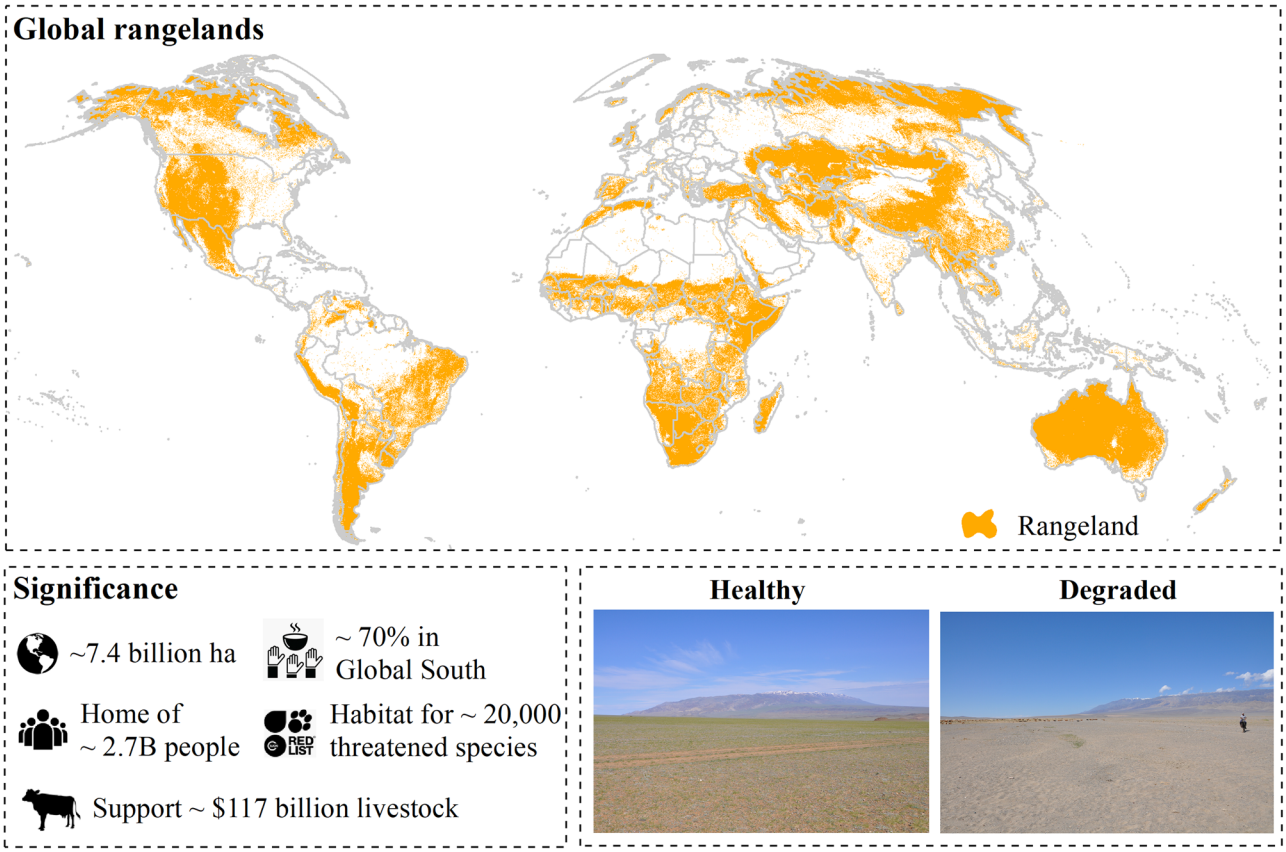

Fig. 1 | Rangelands. Global distribution map (500 m, 2023; MCD12Q1), a snapshot of significance, and examples of healthy vs degraded rangelands in Mongolia.

Productivity (Aus RAPP) platform, drawing on MODIS data, offers broader global coverage[9]. However, it faces limitations due to the inherent constraints of MODIS imagery, including a reduced spatial resolution (500 m) and a shorter temporal span (available since 2000). Meanwhile, other existing methods projecting global rangeland changes rely on modeled data, presenting long-term forecasts at even coarser resolutions (>25 km)[10,11]. Although finer mapping techniques (e.g., ≤30 m pixels) exist for diverse ecosystems (e.g., forests, croplands, and wetlands[12–14]), a comparable high-resolution framework for global rangeland analysis remains absent. Our study aims to bridge this gap, laying the foundation for advanced rangeland monitoring and management strategies (see Table S1).

Rangeland condition tracking needs to be done in a way that can effectively support decision-making for greater sustainability. This is particularly challenging for rangelands which, compared with forests, tend to exhibit fewer natural thresholds (e.g., forest conversion) under their dominant use (grazing) and experience high inter- and intra-annual variability predominantly due to changes in rainfall. Effective decision support therefore requires a flexible but robust statistical approach that can illuminate when changes of concern to decision-makers are observed and how likely these are.

To address the above mentioned gaps in the field, this study developed a novel analytical approach to map rangeland condition changes at 30 m spatial resolution. We illustrated this approach over Mongolian rangelands, which can further extend globally in the future. Based on the new capabilities of the long-term global Landsat image archive, we incorporated dynamic statistical modeling into the proposed approach to track the rangeland condition changes as well as to quantify the likelihood of such changes. Therefore, our approach facilitates the use of accumulated satellite data to monitor multiple levels of change in the rangeland system (as defined by end users) and to identify the support for each level of change given the data. Such information can then be used to quantify management impact and define a level of certainty regarding this impact, delivering improved knowledge for global rangeland management and conservation investments.

Results

Initial status of rangeland condition

Identifying rangeland condition change requires the determination of a prior or initial condition to assess this change against. We used a benchmarking method to identify the condition of rangelands prior to 1990, which quantifies local rangeland productivity relative to the potential productivity in the same Land Capability Class (LCC) of homogeneous lands with similar biogeophysical capability under similar climate conditions. A total of 4918 LCCs were defined across the continent of Asia and 1962 classes over Mongolia (Fig. 2a). Then, we identified areas within each LCC that possessed the minimum (lowest tenth percentile) or maximum (highest tenth percentile) productivity performance possible for the LCC they belonged to (red and green areas respectively in Fig. 2b). Areas in red in Fig. 2b indicate the lowest production relative to their potential, assuming the presence of rangeland vegetation. This suggests that these rangeland areas might have already experienced severe land degradation at the beginning of our study period. As a result, pixels within these regions that have 'stable condition' modeled in our subsequent analysis indicate rangelands that stay consistently degraded during the study time. In contrast, areas in green in Fig. 2b show rangelands with the highest relative production, in other words reaching nearly their full potential within each LCC.

Rangelands varied across Mongolia in their initial conditions relative to the maximum productivity possible within each LCC (Fig. 2c), which present near full productivity potential in the center of the country while reductions in parts of northern and southern Mongolia prior to 1990. In addition, transitions in land cover within Mongolia from 1992 to 2020 were investigated with land cover yearly data and observed to be few, with only a minor proportion of rangelands in the north (almost none in the south) being converted to other land cover types (Fig. 2d). These areas were

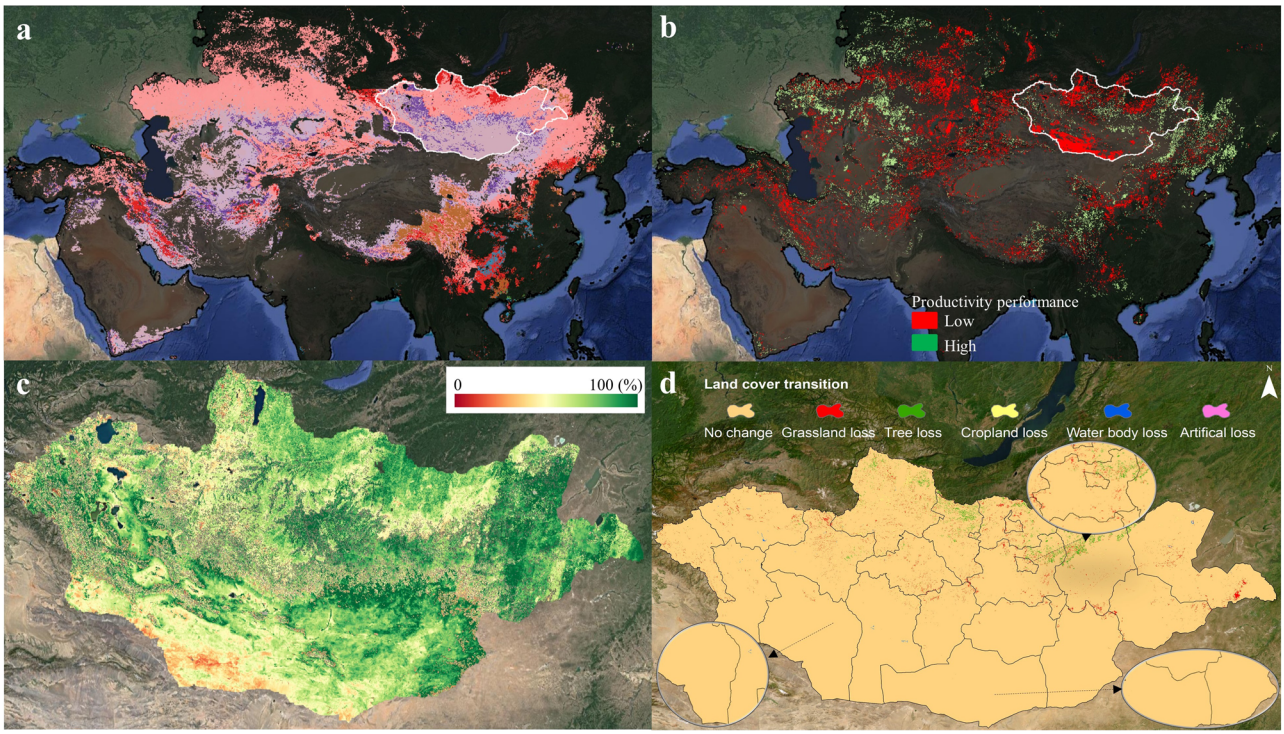

Fig. 2 | Rangeland initial condition. a Land capability classes (n.b., colors are only for illustration purposes and not enough for all LCCs). **b** Extremes of initial rangeland productivity performance (lowest and highest tenth percentiles) across the continent of Asia. **c** Initial rangeland productivity across Mongolia, scaled by their maximum production. **d** Land cover transitions over Mongolia from 1992 to 2020.

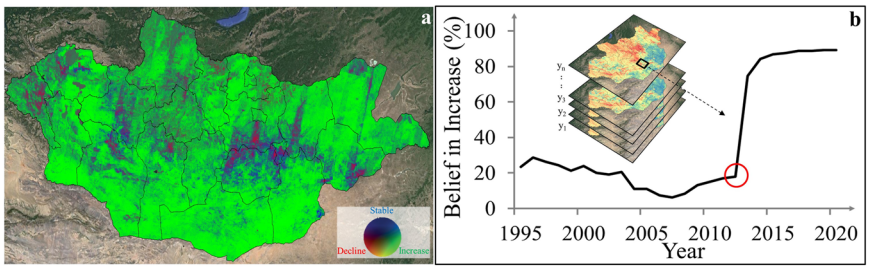

Fig. 3 | Spatio-temporal condition changes of rangelands in Mongolia from 1986 to 2020. a RGB composite map of beliefs in 'increase', 'stable', and 'decline' conditions modeled from the 35-year window of the entire study time (n.b., the vertical stripes were due to the mosaic of satellite image scenes). **b** Map series stack of beliefs in 'increase' from decadal moving-window sliding one year step each time, with each year on the x-axis representing the belief in rangeland productivity increase during its previous 10-year. For example, a dramatic jump in the statistical belief (circle in red) in 2012 shows an improved rangeland condition during 2003–2012.

included in our rangeland condition change analysis but excluded in the process of our management assessment.

Trajectories of rangeland condition change

The spatial distributions of overall changes in rangelands across Mongolia were derived from the 35-year window of the entire study time (1986–2020), and represented by the RGB composited belief images of the three condition models (Fig. 3a). In contrast to the spatial patterns of initial condition that indicated maximum productivity in the center of Mongolia and lower productivity elsewhere prior to 1990 (Fig. 2c), we found rangelands across the center of Mongolia with dense population and intensive grazing activities showed overall higher belief in 'decline' (red areas in Fig. 3a) compared to other areas. Specifically, most of the southern Mongolia desert region, where vegetation dynamics are being driven by climate variability, presented improved rangeland conditions for the past 35 years, with the green color indicating a high belief in 'increase' condition.

The annual time series of statistical beliefs in decline, increase, or stable rangeland status were derived from the accumulated vegetation condition changes during each previous decade (Fig. 3b), which may show details of the overall condition changes geographically presented in Fig. 3a. Such time series of beliefs in condition changes enable quantitative assessment of rangeland management impacts over both large and small areas. For example, the black box indicated in Fig. 3b is a protected area located within an overall improved condition environment. For this protected area there was a dramatic jump in the trajectory of beliefs in 'increase' (red circled point in Fig. 3b), which may indicate the implementation of a successful management intervention in 2012.

Management impacts

We evaluated the impacts of rangeland management within each protected area individually and then synthesized the findings to compare the effectiveness of various management strategies implemented across Mongolia. With the abovementioned map series of beliefs in the 'increase' condition, management impacts were quantified as the difference of beliefs in the 'increase' condition over each protected area between the prior- and post-management periods. Since rangelands have been protected across

Mongolia by three levels of management (National Protected Areas with four sub-management strategies, NPAs; Local Protected Areas, LPAs; and Community-Based Organisation, CBO), we focused our analysis on the country-wide effects of these different management strategies.

The spatial distributions of the belief difference in 'increase' over local protected areas before and after the management are shown in Fig. 4a, with green-colored areas indicating improved rangeland condition after the management while those in red presented no improvement. We found over 74% of the LPAs showed higher belief in the 'increase' condition after the management applied. However, such improvement over a large proportion of the protected areas could have resulted from the combined impacts of both natural climate and human management interventions. Indeed, we found there has been an increasing trend in rainfall across Mongolia since 2011 that may have positively impacted rangelands over the last decade (Fig. 4b). As a result, we need to separate the management impact from those due to inter-annual climatic variability on rangelands to better understand the benefits from rangeland management interventions.

Using all areas under the same LCC as a reference, we removed the rainfall effect by subtracting belief in the 'increase' of protected areas from that of the reference sites for the pre- and post-management periods ("Methods" section). We found after the removal of the rainfall effect, the percentage of local protected areas showing higher belief for the post-management period reduced to around 25% (Fig. 4c). This indicates the ecological improvement in most of the local protected areas was due to climate variability (i.e., rainfall increase) rather than management effects. More specifically, 25% of local protected areas showed condition improvement linked to management, rainfall contributed to the vegetation increase for half of the areas, and the other 25% didn't show significant improvement under either climate or management effect.

Comparison among different management strategies

In contrast to local protected areas, the national protected areas (NPA) presented 100% improvement under the context of both management and climate effects (Fig. 5a); 77% of these benefits were due to management alone after rainfall correction (Fig. 5b). Being both equally distributed across Mongolia, the management of national protected areas outperformed that of the local protected areas, with higher median belief difference in 'increase' and less variance (Fig. 5c). We also found the earlier NPA management establishment was likely to link with higher belief in 'increase' after the management (Fig. 5c). In addition, the protected areas on both levels showed land degradation around Mongolia's capital city of Ulaanbaatar, where intensive grazing activities occur such as areas in the central and eastern grassland as well as northern mountain grassland ecoregions (Figs. 4c and 5b).

The effectiveness of the four different sub-management strategies under the NPA management was also analyzed in this study, including the 'strictly protected area', 'national parks', 'nature reserve', and 'natural and historical monument areas'. We found overall improvement due to all four NPA strategies, with the median belief difference in 'increase' above zero between before and after all the management applied (Fig. 5d). 'Strictly protected areas' were observed to have the most effective management among all four, followed by the 'national parks' while 'nature reserve' and 'natural and historical monument areas' showed relatively lower effectiveness. The improved rangeland condition in the community-based organization areas (highlighted in red polygons in Fig. 5a, b) was observed to be solely attributed to rainfall. However, the management of these areas investigated in our study was only recently implemented (late 2018 and 2020), which likely limited the extent of any potential impact on rangeland conditions.

Discussion

The validation of our rangeland condition changes and management assessments, using a triad of methods informed by field observations and regional reports on Mongolia's rangeland health, yielded coherent results. Firstly, our statistical beliefs in 'increase', 'stable', and 'decline' conditions showed strong spatial concordance with the observed degradation levels across Mongolia (Fig. 6a). For instance, areas with high beliefs in 'decline' predominantly encompassed locations of fully and heavily degraded field

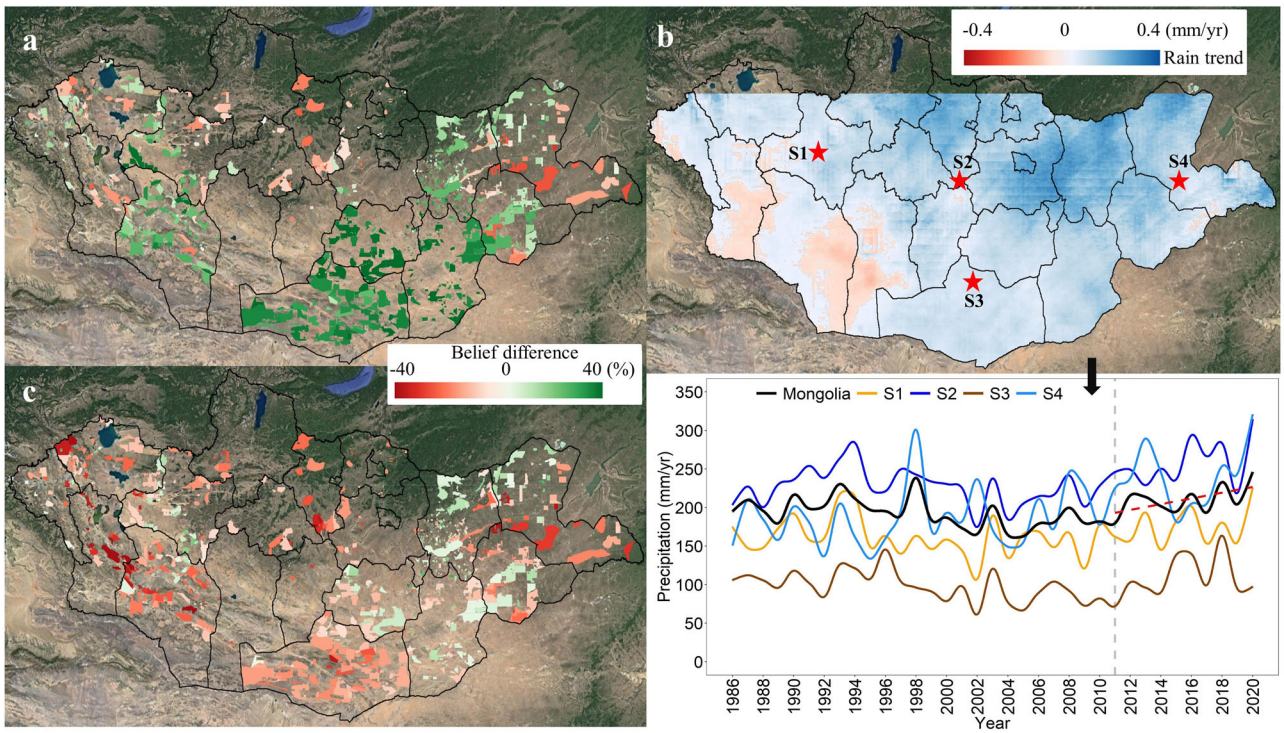

Fig. 4 | Belief difference in 'increase' between the prior- and post-management periods. a Spatial distributions of the combined impacts from management and climatic variability on local protected areas. **b** Annual rate of change in precipitation across Mongolia during 2011–2020, compared to time series of spline-smoothed yearly mean precipitation over four local protected areas (labeled as S1, S2, S3, and S4) from 1986 to 2020. **c** Spatial distributions of the sole management impacts on local protected areas.

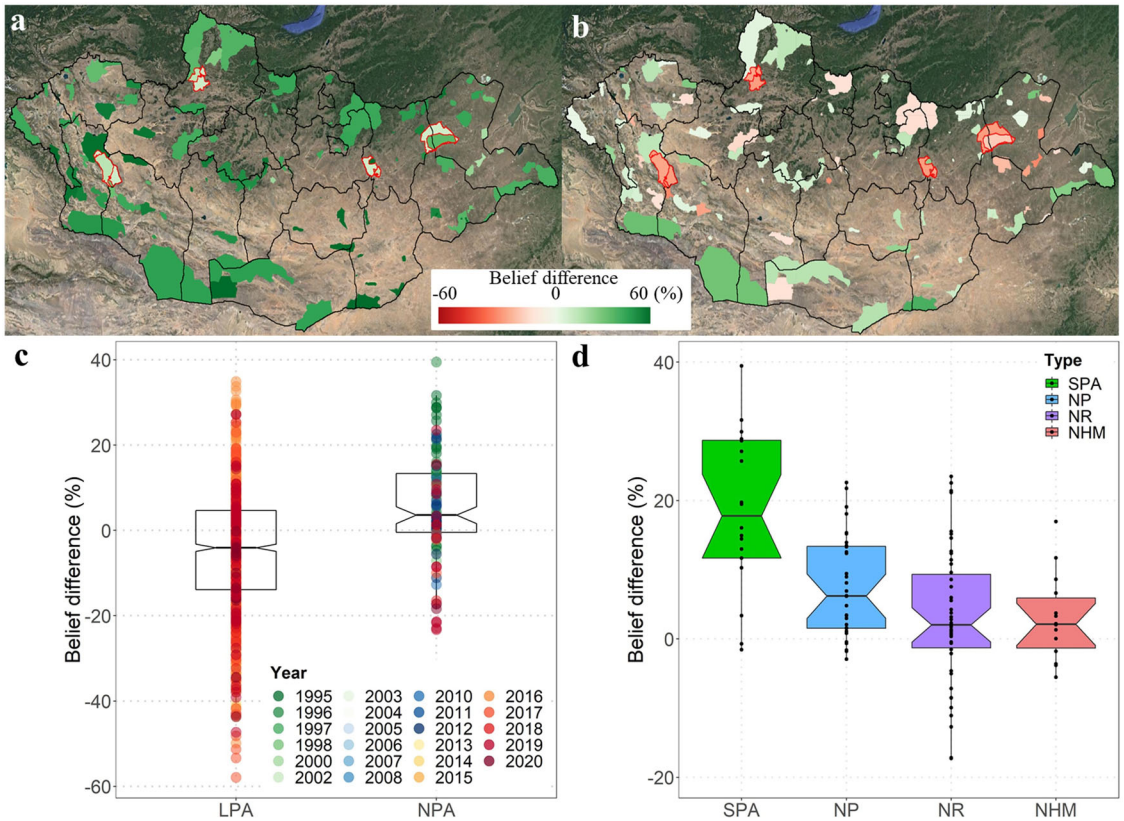

Fig. 5 | Comparison of different management strategies. a Spatial distributions of the combined impacts from management and climatic variability on national protected areas. **b** Spatial distributions of the sole management impacts on national protected areas. Boxplots for **c** local (LPA) and national (NPA) protected areas colored by the time of management establishment and **d** protected areas of the four different management strategies under the NPA management (SPA 'strictly protected area', NP 'national parks', NR 'nature reserve', NHM 'natural and historical monument areas'). Values in (**a**–**d**) are belief differences in 'increase' between the prior- and post-management periods (i.e., after the correction of the climatic effect).

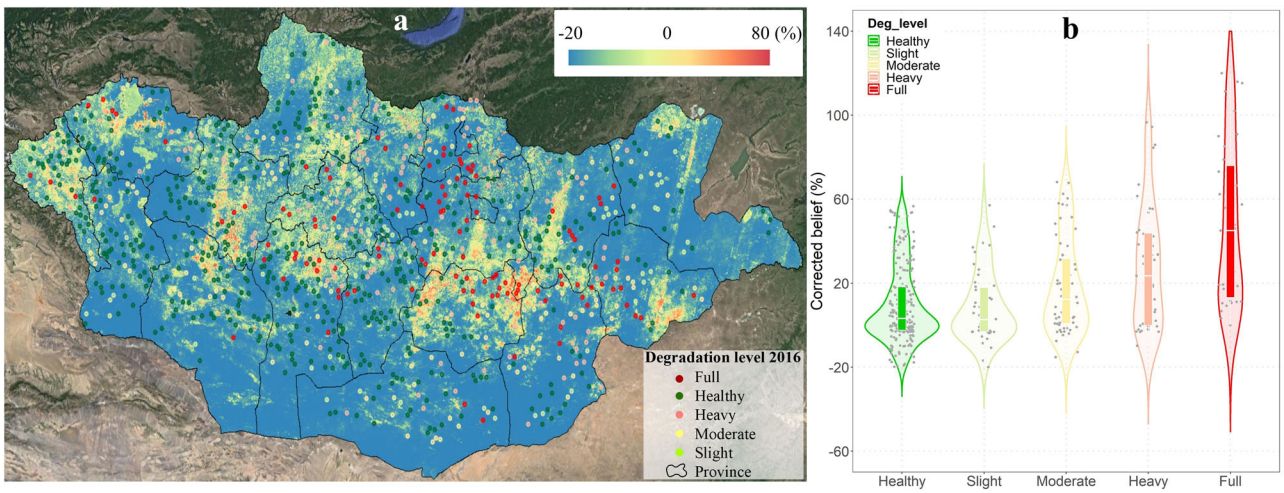

Fig. 6 | Spatial alignment between field observations and mapped rangeland condition changes across Mongolia. a Rainfall corrected belief in the 'decline' map over a 31-year period of 1986–2016 with field observations of five different degradation levels acquired in 2016. **b** Corresponding rainfall corrected beliefs in 'decline' for all the validation points across different degradation levels.

observations, whereas areas with low beliefs in 'decline' largely corresponded with healthy field sites. Furthermore, the density distribution plot of validation points (Fig. 6b), which illustrates the beliefs in 'decline' across different degradation levels, unveiled a discernible pattern: the central tendency and dispersion indicate that areas with more severe degradation observed in the field are associated with higher beliefs in 'decline' in our analysis. Initially, Mongolian rangelands (1986–1990) exhibited minimal productivity reduction in central and eastern regions (Fig. 2c), yet these areas later displayed high beliefs in 'decline' from 1986 to 2016 (Fig. 6a). This shift could be attributed to Mongolia's economic transition post-1990, which saw a surge in subsistence herding and migration towards provinces near Ulaanbaatar due to job losses and a tripling of livestock numbers[15].

Table 1 | Accuracy statistics of the rangeland condition change map from 1986 to 2016 derived from the confusion matrix analysis

	Reference (ground truth)		Accuracy assessment[a], %			
Class	Degradation	Healthy	UA	PA	OA	BA
Degradation	229	91	76.7 (±4.20)	71.7 (±4.32)	79.9 (±2.56)	78.5
Healthy	118	532	81.8 (±2.96)	85.4 (±2.77)		

Standard errors of the estimates are provided in parentheses.
[a]User's Accuracy (UA), Producer's Accuracy (PA), Overall Accuracy (OA) and Balance Accuracy (BA) are described in Table 1.

The confusion matrix analysis underlines our model's proficiency and challenges in classifying rangeland conditions (Table 1). The matrix indicates a User's Accuracy of 76.7% for 'Degradation' and 81.8% for 'Healthy', with corresponding Producer's Accuracies of 71.7% and 85.4%, respectively. This reflects a solid capability in identifying both degraded and healthy rangelands, supported by an Overall Accuracy of 79.9% (±2.56). However, the reduced accuracy observed in the 'Degradation' category underscores the complexities of accurately identifying areas of true degradation. This may be attributed to the limitations of remote sensing to detect early-stage degradation, the masking effects of human activity and climate change on degradation signals, and our preliminary application of basic models with a theoretical 20% threshold for change. This threshold merits adjustment by rangeland managers utilizing their practical insights.

Our results from assessing the impact of different rangeland management strategies showed good agreement with the impacts of management strategies described in the regional reports[16]. For example, the four categories of management applied to the national protected areas varied in their effectiveness with 'strictly protected areas' showing the most benefits to vegetation increase in rangelands followed by 'national parks', which outperformed 'nature reserve' and 'natural and historical monument areas' (Fig. 5d). This is because 'strictly protected areas' and 'national parks' have been managed by different protected area administrations from the other two, the former of which received more funding from the central government to have better governance[16,17]. This was further confirmed by the qualitative assessments of previous government research on the comparison among the four management strategies over different small regions via the Management Effectiveness Tracking Tool developed by WWf[18–20]. In addition, we found the management of national protected areas had much more positive impacts on protected rangelands than that implemented for local protected areas. This may be attributed to the limited financial capacity of local governments (Province and county levels), to provide sufficient funding for the management of local protected areas[17]. As we observed, however, the time since management establishment is an important factor in the rangeland condition trend (Fig. 5c), suggesting some of the differences between national and local protected areas captured here could be attributed to the earlier implementation of the national protected areas. Moreover, results from this study might be subject to uncertainties stemming from data limitations, methodological constraints, and local environmental factors. For example, the use of Land Capability Class, designed to assess agricultural potential based on soil properties, lacks specific linkage to ecosystem functionality or vegetation communities. As global data and methodologies evolve, further efforts are necessary to refine or replace LCC, however, our approach is flexible to such adaptations. Similar to conventional remote sensing methods, our study's focus on the greenness index mainly captures grassland cover changes, possibly missing rangeland areas with significant woody and invasive species encroachment. Future efforts could integrate additional field data on invasive species abundance, and apply ecological models to understand the spread and impact of invasive species on grasslands. In general, the ability to incorporate more diverse data sources will allow for a more comprehensive management impact analysis.

The proposed approach in this study consists of simple but robust statistical algorithms, which can be achieved by satellite observations and spatial products that are globally freely available without being dependent on the field observations. Thus, it has great future potential to extend to a global scale with even higher spatial resolution satellite imagery (e.g., sentinel-2 or planet) via cloud computing platforms such as GEE. In addition, this study enables flexible models of change to be identified. First, the linear percentage change can be replaced by a non-linear if needed. Further, the level of change of interest, e.g., ±20% investigated in this study, is flexible, and any, or multiple, values could be assigned, and more than three models could be identified and assessed within this approach. The assessment window designed in this study is also flexible and could track a single year or any length up to the entire period of the data. There is a well-documented concern with methods that set a binary threshold (e.g., a *p*-value) to assess whether an area is degraded or its condition has changed[21]. This study avoids using such thresholds and instead focuses on likelihoods associated with different extents of change. Avoiding a standardized approach to defining rangeland conditions provides flexibility, so end users can look for changes and levels of confidence in those changes, which reflect their own beliefs and choices about sustainability.

Conclusions

Despite their vast extent and the crucial resources that rangelands provide to people and nature, we currently have a limited accounting of rangeland's condition. In this study, we proposed a novel analytical approach that does not compromise on spatial resolution or time scale and avoids standardized definitions of rangeland condition change. This approach links three features critical for a significant advance in rangeland research: (1) identifying the initial state of rangeland condition before the satellite era; (2) mapping rangeland condition changes and estimating the likelihood of such changes at high spatial resolution (30 × 30 m) over long-time horizons (40 years); and (3) quantifying the impacts of different large-scale management on rangeland condition. Our initial findings show the new approach can be applied over the rangelands of Mongolia to detect and identify landscape changes especially in vegetation cover, at scales that can be used to inform the development and assessment of sustainable rangelands management programs. Details of these management programs need to be regionally specific and are beyond the scope of this work.

Methods

The proposed approach encompasses a four-stage process, as outlined below (Fig. 7), and has been developed utilizing the Google Earth Engine (GEE) platform. The data employed in this study are freely accessible on a global scale, with the majority pre-existing within GEE, while the remainder has been uploaded to the user's asset space on GEE.

Study area

We used Mongolian rangelands as a case study to test our proposed approach, which is an area that covers 80% of the country (over 120 million hectares). Rangelands in Mongolia support approximately one million nomadic herders (30% of the population) and provide refuge for a variety of rare and wide-ranging wildlife[22]. Rangelands may be degrading due to loss of traditional grazing practices, and increases in livestock numbers (tripled during the past three decades), combined with impacts of mining and infrastructure development. The degradation caused by these impacts has been accelerated by climate change and population growth[23]. In recognition

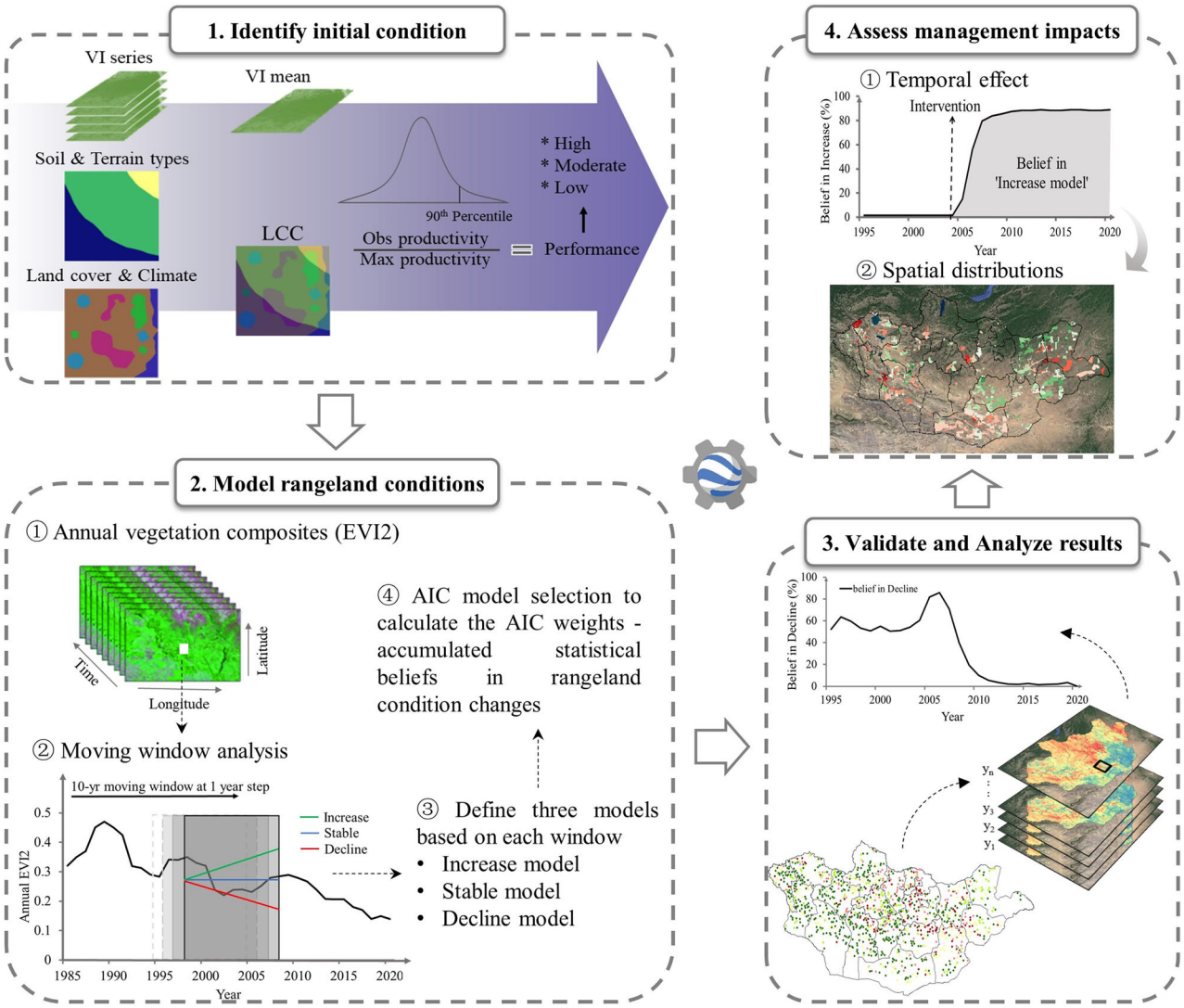

Fig. 7 | Approach flowchart of this study.

Table 2 | Summary of data used in this study

Name	Purpose	Resolution	Time	Source[a]
Landsat	Main data	30 m/annual median	1986–2020	GEE data catalog
Protected areas	Management assessment	NA	1995–2020	TNC Mongolia
Precipitation	Climate assessment	0.05°/annual sum	1986–2020	GEE data catalog
Land cover	land capability classification	300 m/annual	1992–2020	GEE data catalog
Soil units	land capability classification	250 m/NA	NA	GEE data catalog
Terrain	land capability classification	250 m/NA	NA	GEE data catalog
Climate	land capability classification	1 km/annual	1986–2020	GEE data catalog
Field data	Validation	NA	2016	Mongolian Government

[a]Google Earth Engine (GEE) and The Nature Conservancy (TNC) are described in Table 2.

of the importance of sustainable rangeland use, the Mongolian government has been working with The Nature Conservancy to strengthen the management of protected areas to balance conservation and development. Three levels of land protection at different spatial scales, covering most of Mongolia, have been gradually established since the 1990s including National Protected Areas (NPA), Local Protected Areas (LPA), and more recently, Community-Based Organization (CBO) areas[24] (Table 2). The large extent of rangelands with a long-term record of different rangeland management interventions makes Mongolia an ideal region to test our analysis for global rangeland application.

Landsat data and vegetation index selection

We used the entire Landsat archive of surface reflectance data from 1986 to 2020 (Table 2), which have been corrected for atmospheric, reflectance, topographic, and satellite sensor effects[25]. Spatially, 129 Landsat scenes were required from World Reference System path 122–144 and rows 23–31 to

mosaic and cover the entire Mongolia. This resulted in the acquisition of totally over 100,000 images from GEE's median across different Landsat sensors, including the Landsat Thematic Mapper (TM, Landsat 4-5), the Enhanced Thematic Mapper Plus (ETM+, Landsat 7) and the Operational Land Imager (OLI, Landsat 8) at 16 days and 30 m resolutions. The quality assessment flags provided in Tier 1, Collection 1 product were used to remove undesirable elements such as aerosol, cloud, cloud shadow, and inundation[26,27].

Initially vegetation index, as a biophysical measure for changes in the amount of green vegetation/photosynthesis in rangelands[28,29], was used in this analysis to demonstrate the feasibility of the research design and approach over the spatial and temporal scales. This will provide a basis to transition to other products such as vegetation fractional cover, which with the inclusion of field observations may be more effectively linked to local management activities but are not currently available at high resolution and globally[9]. The Enhanced Vegetation Index (EVI) was developed as an alternative vegetation index of the Normalized Difference Vegetation Index (NDVI) with reduced soil and atmospheric influences and improved sensitivity in high biomass regions[30]. However, EVI requires a blue band, which can be sensitive to variations in the viewing geometry, surface albedo, sun angle, and terrain[31]. For example, here we found such erratic blue behavior often causes upward spikes in EVI over many parts of Mongolia. To address this issue, we chose to use two-band EVI2 as a surrogate of EVI to avoid data noise over complex environments such as landscapes in Mongolia. EVI2 has been proven to be a good indicator for above-ground biomass[32], which has been widely used for Mongolian rangeland studies[33,34]. EVI2 was calculated as below[35]:

$$\mathrm{EVI2} = 2.5 \times \frac{\rho_{nir} - \rho_{red}}{\rho_{nir} + 2.4 \times \rho_{red} + 1} \quad (1)$$

Where ρ_{nir} and ρ_{red} represent surface reflectance in the near-infrared and red bands. Annual composites of EVI2 for the period of 1986–2020 were then computed for this analysis based on the median of the year, which is a specific data point instead of an averaged or blended value and robust against extreme values and outliers[25].

Management data

Rangeland protected area data provided by TNC Mongolia was used for management assessment in this study, which was applied during the last three decades to balance conservation and development in Mongolia (Table 2). They are under three levels of management strategies, including National Protected Areas (NPA), Local Protected Areas (LPA), and Community-Based Organization areas (CBO). The Mongolian government aims to establish 30% of the country's land as national protected areas and has already reached 20%. TNC Mongolia has been collaborating with the TNC's global team over the past decade to conduct ecoregional assessments and landscape-level planning across Mongolia, helping central and local governments to establish new protected areas. Traditional grazing of livestock is currently allowed in all local protected areas and in parts of national protected areas except the strictly protected NPAs. In addition, the Mongolian government and TNC support local communities to actively participate in the development of rangeland management plans within local protected areas and CBO areas (in many cases these areas overlap). Communities can improve local rangeland management by implementing their traditional sustainable grazing practices, limiting the inflow of herders from other areas, and preventing the establishment of new mining concessions.

Precipitation

We obtained daily precipitation data on GEE from Climate Hazards Group InfraRed Precipitation with Station data (CHIRPS) to assess the interannual climatic variability over Mongolia (Table 2). CHIRPS is a quasi-global rainfall dataset from 1986 to the present, spanning 50°S–50°N[36,37]. It incorporates 0.05° resolution satellite imagery with in-situ station data to create gridded rainfall time series suitable for trend analysis and seasonal drought monitoring. Annually summed precipitation time series were used in this analysis.

Biogeophysical data and land capability classification

'Land capability' is a widely used concept in agricultural science, indicating the suitability of the land for a specific use such as rangeland or rain-fed cultivation[38]. We used Land Capability Class (LCC) to form the basis for identifying the rangeland initial condition, which represents areas with similar land capability under homogeneous biogeophysical and climatic environments (Table 2). K-Means clustering, which is an unsupervised machine learning algorithm, was used to classify the LCCs based on unique and comprehensive layers of independent variables with all data available at a global scale. This data included: *Land cover* - Land cover map at 300 m resolution with 22 major classes from 1992 to 2020 provided by the ESA Climate Change Initiative[39], which was derived from five different satellite missions based on the United Nations land cover classification system; *Soil units* - soil taxonomy at 250 m with 12 classes[40], which is distribution of the USDA soil great groups based on machine learning predictions from global compilation of soil profiles (>350,000 training points); *Terrain* - landform at 250 m with 5 major classes produced using the improved Hammond Landform Classification Algorithm[41]; *Climate* - Koppen-Geiger climate zones at 1 km resolution for the period of 1986–2020[42], which was derived from an ensemble of 32 climate models based on temperature, precipitation, potential evapotranspiration, etc with 13 major classes (at 1st and 2nd levels).

Initial rangeland condition identification

Being confined by the satellite lifespan, remote sensing methods can only detect lands that have been actively affected by the ongoing processes of degradation since the 1980s[43]. This means rangelands with the initial condition of severe land degradation may show little decline during the satellite time. As such, identifying the initial condition of rangelands is the crucial first step for a better understanding of the changes in the condition of these lands during our study period. To do this, the Local Net Production Scaling (LNS) was used[44], which as a benchmarking method works on condition that: (1) it is based on the LCC with the same rangeland productivity level, and (2) non-degraded reference sites exist in each LCC. We thus defined LCC over the whole continent of Asia instead of Mongolia to ensure there are enough reference sites. The LNS index was calculated across the averaged annual EVI2 image over the first five years of the study time (1986–1990), which was derived by scaling the actual EVI2 of each pixel relative to the higher observed EVI2 value in the frequency distribution of all pixels in the same LCC. The areas with full potential and minimum productivity performance of each LCC class were estimated by the EVI2 values at 90th and 10th percentiles. We set the LNS index of pixels with EVI2 being in the bottom and top 10th percentiles to 0 and 100 respectively to reduce the effect of very high or very low annual EVI2 values caused by atypical areas with low frequency (e.g., unmapped cultivation or bare rock). The LNS index of the other pixel percentiles was scaled linearly between these limits as follows[38,45]:

$$\begin{aligned} &\text{If } qi \le q0.1, \mathrm{LNS}_i = 0; \text{ or} \\ &\text{If } qi \ge q0.9,\ \mathrm{LNS}_i = 100; \text{ or} \\ &\text{If } q0.1 \le qi \le q0.9, \mathrm{LNS}_i = 100\,(qi - q0.1)/(q0.9 - q0.1); \end{aligned} \quad (2)$$

where $q_{0.1}$, $q_{0.9}$ and q_i are EVI2 values at 10th, 90th and in between percentiles respectively.

Then, areas with LNS < = 10 present the lowest production relative to their capability, i.e., already under severe land degradation at the start of our study period. As a result, we set the belief in 'decline' as 100% for pixels within these areas that have 'stable condition' modeled in our following analysis, indicating rangelands under consistent degradation during the study time instead of being stable.

Rangeland condition change modeling

We defined three rangeland condition models at each Landsat pixel location area (30 × 30 m) to represent the significant change (decline/increase) and stable conditions of rangelands (Fig. 2). Previous studies showed 10–20% reduction in land productivity (represented by vegetation greenness) was observed between degraded and non-degraded areas within arid and semi-arid regions[46,47]. Therefore, the three models for Mongolian rangelands in this analysis were expressed as simple linear equations, i.e., 20% decline or 20% increase or similar as mean from the start to the end of the study period:

$$\begin{aligned} &\text{If Model}_{\text{increase}}, z = -20\%; \\ &\text{If Model}_{\text{decline}}, z = 20\%; \text{and} \\ &\text{If Model}_{\text{stable}}, z = 0. \\ &\text{Then } y = y_m \times \left(1 + t \times \frac{z}{T}\right) \end{aligned} \quad (3)$$

Where y represents the predicted EVI2 value, y_m is the mean of annual EVI2 during the study period, t is time at the yearly step, and T is the end year of the study period. The threshold z for the significant change can be modified according to the local environment by end users in the future.

The three defined rangeland condition models were further applied through a moving-window method, which shifts a kernel of the 10-year period over the EVI2 time series of each pixel, sliding one year step each time to create an annual belief time series from 1995 to 2020. This allowed candidate condition models to be dynamically built at each window to model the rangeland condition changes over time. Rather than the traditional null hypothesis testing approach with an arbitrary probability threshold (e.g., *P-value* < 0.05) that is normally used[48], this study used a formal model selection procedure to identify the relative support for each of the three models described in Eq. (3), given a 10-year time series of EVI2 values for each pixel. Specifically, Akaike Information Criterion (AIC) weights were calculated for each of the three competing models to provide a quantitative measure of belief (scaled between 0 and 1; all beliefs sum to 1) for each rangeland condition hypothesis[49]. AIC uses maximum likelihood scores as a measure of fit, enabling inference to be drawn from multiple candidate models simultaneously. Thus, with each 10-year moving window, rangeland condition change was calculated at pixel level across Mongolian rangelands. The derived time series of three weights represents the relative likelihood of the condition change type, indicating the statistical beliefs in decline, increase or stable rangeland status from the accumulated vegetation condition changes during each previous decade.

Accuracy assessment

Field observations of rangeland conditions across Mongolia for validating our results were collected from a nationwide rangeland survey program by the National Agency for Meteorology and Environmental Monitoring (NAMEM) in 2016, covering most of the vegetation types at 1040 monitoring sites across the country. The NAMEM further converted the observations to 5 different degradation levels by using an interpretation tool named Ecological Site Descriptions. These degradation levels were carefully established by comparing the vegetation health at each site against that of healthy counterparts within the same specific vegetation communities. They describe a sequence of changes from healthy rangeland conditions toward unproductive states based on key criteria such as species composition, bare soil cover, total species number, the proportion of palatable and degradation indicator species, litter accumulation, and above-ground biomass (details in Table 3).

The accuracy assessment of this study was carried out using both qualitative and quantitative methods based on field data. Qualitatively, we examined the spatial coherence between field observations and changes in rangeland conditions depicted in the map, alongside its concurrence with local environmental and management reports. Quantitatively, we employed a confusion matrix to calculate Overall Accuracy (OA), Producer's Accuracy (PA), User's Accuracy (UA), and Balanced Accuracy (BA). In constructing the confusion matrix, we generated a dominant rangeland condition change map from 1986 to 2016 using the maximum value rule across beliefs in "Increase", "Stable", and "Decline" maps. To harmonize the five degradation levels from field data with the three categories on our rangeland change map, we grouped them into two classifications: "Healthy" and "Slightly degraded" levels from field observations, along with "Increase" or "Stable" conditions from our map, were designated as the "Healthy" class; conversely, "Moderately degraded", "Heavily degraded", and "Fully degraded" levels from field data, matched with the "Decline" condition from our map, were classified as the "Degradation" class.

Separation of natural variability from rangeland management impacts

Changes in rangeland condition represented as a belief in the support of the data for different models of change (i.e., decline, increase, and stable) were output as time series over a 10-year moving window and over the whole study period (1986–2020) for each pixel. These trajectories serve as a foundation for exploring condition change in rangelands under differing perspectives, including tracking historical trajectories and spatial patterns of rangeland change in response to different land management decisions. Here we utilized the time series of belief in 'increase' to quantify the effectiveness and spatial distribution of benefits associated with protected area policies across Mongolia.

To ensure the difference observed pre- and post-management periods from these belief trajectories represents a signature of the management and not inter-annual climatic variability inherent in rangeland systems, it was essential to remove the impact of this variability from the trajectories. Such a need has been recognized in previous studies[50,51]. The most common method, Residual Trends Analysis (RESTREND), compares expected plant growth based on rainfall patterns with actual satellite observations to remove the effects of climate variability. However, this method has been proven unreliable when the change observed is greater than 20%[46]. Given our study aims to be flexible to the level of change to be detected, to complement targets, decision triggers, or reporting needs of many end users in these vast rangeland systems, we had to explore another approach. We instead utilized a method based on LCC to isolate the effects of human management[38,44].

To remove the rainfall variability from our belief calculation, we developed a continental scale reference value for each LCC across Asia for comparison with the managed areas in this study, in this case, protected area declaration and management. By subtracting the belief in an 'increase' in condition after protection with the average for all corresponding reference sites over the same time horizon, we effectively removed rainfall variability and allowed change to be more likely a signature of management implemented. The difference in the belief of an increase in protected areas was mapped to show the spatial distribution of the management impact, as well

Table 3 | The basic criteria followed to classify the field observations of rangeland conditions to 5 degradation levels

Degradation levels	Criteria
Healthy	All native dominants are in place.
Slightly degraded	Key dominants are still dominating, some grazing-sensitive forbs are in decline and grazing-resistant species are in increase.
Moderately degraded	Dominants are in decline and replaced by other subdominants, number of species drops down.
Heavily degraded	Remnants of key species are thinning, and the abundance of degradation indicator species increases.
Fully degraded	Total vegetation cover is reduced or dominated by very few degradation indicator species.

as maps of belief when climate variability is not removed (Figs. 4 and 5). Additionally, land cover changes, such as transitions from rangeland to other land types or vice versa, were identified and excluded from the management assessment analysis. This step was taken to prevent any misattribution of changes in rangeland conditions.

Data availability

All the datasets used in this study are freely and globally available on either Google Earth Engine Data Catalog (https://developers.google.com/earth-engine/datasets/) or their official websites.

Code availability

Google Earth Engine code that was used for data analysis and map display in this study can be accessed via Zenodo https://doi.org/10.5281/zenodo.10806820.

Received: 27 November 2023; Accepted: 18 June 2024;
Published online: 25 June 2024

References

1. Reeves, M. C. et al. Global view of remote sensing of rangelands: evolution, applications, future pathways. In *Land Resources Monitoring, Modeling, and Mapping with Remote Sensing, Remote Sensing Handbook* (CRC Press, 2015).
2. Godde, C. M., Garnett, T., Thornton, P. K., Ash, A. J. & Herrero, M. Grazing systems expansion and intensification: drivers, dynamics, and trade-offs. *Glob. Food Secur.* **16**, 93–105 (2017).
3. Fargher, J., Howard, B., Burnside, D. & Andrew, M. The economy of Australian rangelands—myth or mystery? *Rangel. J.* **25**, 140–156 (2003).
4. Montanarella, L., Scholes, R. & Brainich, A. The Assessment Report on Land Degradation and Restoration (IPBES secretariat, Bonn, Germany, 2018).
5. IUCN. The IUCN Red List of Threatened Species. Version 2020-2 https://www.iucnredlist.org (2020).
6. Kimiti, D. W., Hodge, A.-M. C., Herrick, J. E., Beh, A. W. & Abbott, L. E. Rehabilitation of community-owned, mixed-use rangelands: lessons from the Ewaso ecosystem in Kenya. *Plant Ecol.* **218**, 23–37 (2017).
7. Dror, D. K. & Allen, L. H. The importance of milk and other animal-source foods for children in low-income countries. *Food Nutr. Bull.* **32**, 227–243 (2011).
8. Jones, M. O. et al. Innovation in rangeland monitoring: annual, 30 m, plant functional type percent cover maps for U.S. rangelands, 1984–2017. *Ecosphere* **9**, e02430 (2018).
9. Hill, M. J. & Guerschman, J. P. The MODIS global vegetation fractional cover product 2001–2018: characteristics of vegetation fractional cover in grasslands and Savanna woodlands. *Remote Sens.* https://doi.org/10.3390/rs12030406 (2020).
10. Godde, C. M. et al. Global rangeland production systems and livelihoods at threat under climate change and variability. *Environ. Res. Lett.* https://doi.org/10.1088/1748-9326/ab7395 (2020).
11. Boone, R. B., Conant, R. T., Sircely, J., Thornton, P. K. & Herrero, M. Climate change impacts on selected global rangeland ecosystem services. *Glob. Chang. Biol.* **24**, 1382–1393 (2018).
12. Hansen, M. C. et al. High-resolution global maps of 21st-century forest cover change. *science* **342**, 850–853 (2013).
13. Pekel, J.-F., Cottam, A., Gorelick, N. & Belward, A. S. High-resolution mapping of global surface water and its long-term changes. *Nature* **540**, 418–422 (2016).
14. Zhang, M. et al. GCI30: a global dataset of 30 m cropping intensity using multisource remote sensing imagery. *Earth Syst. Sci. Data* **13**, 4799–4817 (2021).
15. Leisher, C., Hess, S., Boucher, T. M., Beukering, P. & Sanjayan, M. Measuring the impacts of community-based grasslands management in Mongolia's Gobi. *PLoS ONE* **7**, e30991 (2012).
16. Batkhuyag, B. et al. *Sixth National Report to the Convention on Biological Diversity (2015-2018)* 1–168 (Ministry of Environment and Tourism of Mongolia, Ulaanbaatar, 2019).
17. Batjargal, Z. & Shiirevdamba, T. *Expanding the Protected Area Network in Mongolia: A Review and Assessment Report* (TNC Mongolia, 2017).
18. Stolton, S. & Dudley, N. *METT Handbook: A Guide to Using the Management Effectiveness Tracking Tool (METT)* (WWF-UK, Woking, 2016).
19. Dudley, N. et al. *Tracking Progress in Managing Protected Areas Around the World* (WWF International, Gland, 2007).
20. Namsrai, O. et al. Evaluating the management effectiveness of protected areas in Mongolia using the management effectiveness tracking tool. *Environ. Manag.* **63**, 249–259 (2019).
21. Halsey, L. G., Curran-Everett, D., Vowler, S. L. & Drummond, G. B. The fickle P value generates irreproducible results. *Nat. Methods* **12**, 179–185 (2015).
22. Ahlborn, J. et al. Climate–grazing interactions in Mongolian rangelands: effects of grazing change along a large-scale environmental gradient. *J. Arid Environ.* **173**, 104043 (2020).
23. Jamsranjav, C. et al. Applying a dryland degradation framework for rangelands: the case of Mongolia. *Ecol. Appl.* **28**, 622–642 (2018).
24. Reading, R. P., Wingard, G., Selenge, T. & Amgalanbaatar, S. *Protecting the Wild* 257-265 (Springer, 2015).
25. Flood, N. Seasonal composite Landsat TM/ETM+ images using the medoid (a multi-dimensional median). *Remote Sens.* **5**, 6481–6500 (2013).
26. Goodwin, N. R., Collett, L. J., Denham, R. J., Flood, N. & Tindall, D. Cloud and cloud shadow screening across Queensland, Australia: an automated method for Landsat TM/ETM+ time series. *Remote Sens. Environ.* **134**, 50–65 (2013).
27. Xie, Z. et al. Seasonal dynamics of fallow and cropping lands in the broadacre cropping region of Australia. *Remote Sens. Environ.* **305**, 114070 (2024).
28. Gonzalez-Roglich, M. et al. Synergizing global tools to monitor progress towards land degradation neutrality: trends.Earth and the world overview of conservation approaches and technologies sustainable land management database. *Environ. Sci. Policy* **93**, 34–42 (2019).
29. Noojipady, P., Prince, S. D. & Rishmawi, K. Reductions in productivity due to land degradation in the drylands of the southwestern United States. *Ecosyst. Health Sustain.* **1**, 1–15 (2015).
30. Huete, A. et al. Overview of the radiometric and biophysical performance of the MODIS vegetation indices. *Remote Sens. Environ.* **83**, 195–213 (2002).
31. Ma, X. et al. Sun-angle effects on remote-sensing phenology observed and modelled using himawari-8. *Remote Sens.* **12**, 1339 (2020).
32. Li, Z. et al. Comparison and transferability of thermal, temporal and phenological-based in-season predictions of above-ground biomass in wheat crops from proximal crop reflectance data. *Remote Sens. Environ.* https://doi.org/10.1016/j.rse.2022.112967 (2022).
33. Otgonbayar, M., Atzberger, C., Chambers, J. & Damdinsuren, A. Mapping pasture biomass in Mongolia using partial least squares, random forest regression and Landsat 8 imagery. *Int. J. Remote Sens.* **40**, 3204–3226 (2019).
34. Matongera, T. N., Mutanga, O., Sibanda, M. & Odindi, J. Estimating and monitoring land surface phenology in rangelands: a review of progress and challenges. *Remote Sens.* **13**, 2060 (2021).
35. Jiang, Z., Huete, A. R., Didan, K. & Miura, T. Development of a two-band enhanced vegetation index without a blue band. *Remote Sens. Environ.* **112**, 3833–3845 (2008).
36. Funk, C. et al. The climate hazards infrared precipitation with stations—a new environmental record for monitoring extremes. *Sci. Data* **2**, 1–21 (2015).

37. Jia, M. et al. Nighttime light in China's coastal zone: the type classification approach using SDGSAT-1 Glimmer Imager. *Remote Sens. Environ.* **305**, 114104 (2024).
38. Wessels, K., Prince, S. & Reshef, I. Mapping land degradation by comparison of vegetation production to spatially derived estimates of potential production. *J. Arid Environ.* **72**, 1940–1949 (2008).
39. ESA. Land Cover CCI Product User Guide Version 2. Tech. Rep. maps.elie.ucl.ac.be/CCI/viewer/download/ESACCI-LC-Ph2-PUGv2_2.0.pdf (2017).
40. Hengl, T. et al. SoilGrids250m: global gridded soil information based on machine learning. *PLoS ONE* **12**, e0169748 (2017).
41. Karagulle, D. et al. Modeling global Hammond landform regions from 250-m elevation data. *Trans. GIS* **21**, 1040–1060 (2017).
42. Beck, H. E. et al. Present and future Koppen-Geiger climate classification maps at 1-km resolution. *Sci. Data* **5**, 180214 (2018).
43. Gibbs, H. & Salmon, J. Mapping the world's degraded lands. *Appl. Geogr.* **57**, 12–21 (2015).
44. Prince, S., Becker-Reshef, I. & Rishmawi, K. Detection and mapping of long-term land degradation using local net production scaling: application to Zimbabwe. *Remote Sens. Environ.* **113**, 1046–1057 (2009).
45. An, R. et al. Monitoring rangeland degradation using a novel local NPP scaling based scheme over the "Three-River Headwaters" region, hinterland of the Qinghai-Tibetan Plateau. *Quat. Int.* **444**, 97–114 (2017).
46. Wessels, K. J., Van Den Bergh, F. & Scholes, R. Limits to detectability of land degradation by trend analysis of vegetation index data. *Remote Sens. Environ.* **125**, 10–22 (2012).
47. Wessels, K. J., Prince, S. D., Carroll, M. & Malherbe, J. Relevance of rangeland degradation in semiarid northeastern South Africa to the nonequilibrium theory. *Ecol. Appl.* **17**, 815–827 (2007).
48. Johnson, J. B. & Omland, K. S. Model selection in ecology and evolution. *Trends Ecol. Evol.* **19**, 101–108 (2004).
49. Akaike, H. *Selected Papers of Hirotugu Akaike* 199–213 (Springer, 1998).
50. Evans, J. & Geerken, R. Discrimination between climate and human-induced dryland degradation. *J. Arid Environ.* **57**, 535–554 (2004).
51. Wessels, K. J., Prince, S., Frost, P. & Van Zyl, D. Assessing the effects of human-induced land degradation in the former homelands of northern South Africa with a 1 km AVHRR NDVI time-series. *Remote Sens. Environ.* **91**, 47–67 (2004).

Acknowledgements

This work was supported by the Australian Research Council Discovery Project (ARC-DP170101480), the Natural Science Foundation of China (42371311), and the Royal Society International Exchanges Cost Share (NSFC 223287). E.M.M. was supported by an ARC Future Fellowship and M.P.A. was funded by an Australian Research Council Discovery Early Career Researcher Award (DE200100683). We thank Adam Charette-Castonguay for providing suggestions on some of the datasets used in this study.

Author contributions

E.M.M., E.T.G., S.R.P., and Z.X. conceived the initial idea. Z.X. performed the analysis and wrote the manuscript with the support of E.M.M., E.T.G., S.R.P., D.J.P., R.J.H., and J.Y., M.P.A. helped with the statistical modeling and associated coding. Y.B., G.P., and B.B. provided Mongolian rangeland management data and suggestions on management assessment. All authors contributed to the writing and revisions of the manuscript on their specific expertise.

Competing interests

The authors declare no competing interests.

Additional information

Supplementary information The online version contains supplementary material available at https://doi.org/10.1038/s43247-024-01516-2.

Correspondence and requests for materials should be addressed to Zunyi Xie.

Peer review information *Communications Earth & Environment* thanks Richard Kingsford and Jian Sun for their contribution to the peer review of this work. Primary Handling Editors: Huai Chen, Joe Aslin and Aliénor Lavergne. A peer review file is available.